



EVALUATION OF P-DELTA EFFECTS IN NON-DETERIORATING MDOF STRUCTURES FROM EQUIVALENT SDOF SYSTEMS

Christoph ADAM¹, Luis F. IBARRA², Helmut KRAWINKLER³

SUMMARY

This paper addresses the assessment of destabilizing effects of gravity, usually referred to as P-Delta effects, in highly inelastic structures when subjected to seismic excitations. The proposed approach is based on an equivalent single-degree-of-freedom (ESDOF) system of the actual building. Appropriate properties of the ESDOF system are defined, based on results of a corresponding global pushover analyses. P-Delta effects are incorporated via an auxiliary backbone curve, which is rotated by a uniform stability coefficient. The procedure is evaluated for several multistory generic frame structures. The collapse capacity of these structures is derived from a set of Incremental Dynamic Analysis (IDA) studies involving 40 ground motions whose intensity is increased until P-Delta instability occurs. The results are translated from the ESDOF domain into the domain of the multi-degree-of-freedom (MDOF) system, and utilized for the estimation of P-Delta effects in MDOF structures. "Exact" results are contrasted with outcomes of the analyses utilizing ESDOF systems. Assumptions and limitations of the ESDOF system approach are discussed. The emphasis is on the level of response at which the structure approaches dynamic instability (sidesway collapse).

INTRODUCTION

Gravity loads lead to a reduction of the lateral stiffness of buildings. Generally, for elastic structural behavior, the decrease is of minor importance in realistic buildings because its magnitude is small compared to the first order elastic stiffness. During severe seismic excitations, however, inelastic deformations combined with gravity may cause a structure to approach a state of dynamic instability if the post-yield tangent stiffness becomes negative. In such a condition, the displacement response tends to amplify in a single direction due to the ratcheting effect, and as a result, the global collapse capacity of the structure is attained at a rapid rate. Studies of the effect of gravity on the inelastic seismic response of structures have been recently presented in [1 - 6].

Equivalent single-degree-of-freedom (ESDOF) systems are used extensively in current design practice to estimate global strength, stiffness, and ductility requirements for multi-degree-of freedom (MDOF)

¹ Assoc. Professor, Vienna University of Technology, Austria. Email: ca@allmech.tuwien.ac.at

² Senior Research Engineer, Southwest Research Institute, USA. Email: libarraolivas@swri.org

³ Professor, Stanford University, USA. Email: krawinkler@stanford.edu

structures. Properties of ESDOF systems have been proposed by several investigators through various formulations (see e.g. [7 - 11]), but the common assumption in most (not all) of the methods is that the deflected shape of the MDOF system can be represented by a shape vector, which remains constant during the time history, regardless of the level of deformation. Application of ESDOF systems for the seismic response prediction of MDOF frame structures is highly desirable in order to customize the extensive database of single-degree-of-freedom (SDOF) systems for these more general structural systems. Because P-Delta effects are mostly controlled by lateral displacements in the lower stories, it is reasonable to assume that these effects can be captured by means of ESDOF systems even in tall buildings in which upper stories are subjected to significant higher mode effects.

The P-Delta effect varies over the height of the structure as a function of the axial force demand and the interstory drift. If the story drifts remain rather uniformly distributed over the height, regardless of the extent of inelastic behavior, then a global assessment of P-Delta is not difficult. However, if a partial mechanism develops, which may extend over one or several stories, then the effective P-Delta effect will be greatly affected by the change in deflected shape, and it will be amplified in those stories in which the drift becomes large. This will affect the effective P-Delta stability coefficient that should be employed in the ESDOF system. Bernal [12] and Aydinoglu [13] have provided good insight into this problem. However, adequate incorporation of P-Delta effects in these ESDOF systems becomes a challenging task for highly inelastic systems.

In real (not equivalent) SDOF systems the effect of P-Delta on the force-displacement relation can be simply modeled by a uniform rotation of the entire hysteretic loop by means of the elastic stability coefficient. In general, the concept of rotation of the hysteretic loop by means of the elastic stability coefficient is also applied to ESDOF systems, see e.g. [14, 15]. However, when structures respond highly inelastic and the P-Delta effects become large the elastic and inelastic stability coefficients may be very different [2]. In these cases, a formulation based only on the elastic stability coefficient is unable to capture the inelastic response because the effective post-yielding stiffness is underestimated. Bernal [12, 16] has suggested to consider P-Delta effects in the ESDOF model by assigning an "average" stability coefficient to the backbone curve of the ESDOF system, which is composed of an elastic stability coefficient assuming a straight deflected shape, and an inelastic stability coefficient associated with the shape of the mechanism at collapse. The shape at collapse is determined from a static pushover analysis, and for both the elastic and inelastic stability coefficient analytical expressions are given by Bernal [16]. In this approach the strain hardening and strength deterioration at critical regions are not included. Furthermore, it is often cumbersome to identify the mechanism involved in P-Delta collapse because not only the global pushover curve (base shear versus roof displacement) must be determined, but also the story drifts of all stories are to be recorded and subsequently evaluated.

In this paper, an alternative procedure for considering P-Delta effects in ESDOF systems is proposed to simplify the derivations of the ESDOF system properties. Appropriate parameters of ESDOF systems are defined rigorously. The shape vector, yield displacement, and post yield stiffness ratio are tuned to results from a global pushover of the corresponding MDOF structure with and without gravity. Elastic and inelastic stability coefficients are derived directly from the roof displacement versus base shear relation without specification of their analytical expressions. The underlying assumption of this procedure is that the post-yielding global stiffness, obtained from the roof displacement vs. base shear relationship, reflects the impact of the global or local mechanism involved when the structure approaches dynamic instability. Consideration of strain hardening is no additional effort, which is another advantage of the proposed procedure. The basic difference with respect to current methodologies is the explicit consideration of the inelastic stability coefficient.

The objective is to assess the extent to which the collapse capacity of regular MDOF structures can be derived from results of the proposed ESDOF system. To achieve this objective, collapse capacities are computed for selected MDOF structures and their corresponding ESDOF models, and the errors in the ESDOF model predictions are evaluated. The collapse capacities are derived from a set of Incremental Dynamic Analysis (IDA) studies involving 40 ground motions whose intensity is increased until P-Delta instability occurs. The results of this investigation are valid only for non-deteriorating hysteresis systems, i.e., strength and stiffness deterioration due to excessive deformations or cyclic loading is not considered.

THE EQUIVALENT SINGLE-DEGREE-OF-FREEDOM (ESDOF) MODEL

Structural modeling of the ESDOF system

Starting point of the subsequent considerations is the governing set of differential equations of an MDOF structural system given as

$$\mathbf{M}\ddot{\mathbf{x}} + \mathbf{q} = -\mathbf{M}\mathbf{r}a_g \quad (1)$$

where \mathbf{M} is the mass matrix, \mathbf{x} denotes the vector of the dynamic degrees of freedom, i.e. displacements relative to the base and rotations, and \mathbf{r} is the influence vector representing the quasi-static displacements of the degrees of freedom from a unit support displacement in direction of the ground acceleration a_g . \mathbf{q} is the vector of internal forces. The deflected shape of the MDOF system is represented by a shape vector, ϕ , which remains constant during the time history, regardless of the level of deformation. The appropriate choice of ϕ is discussed in a subsequent section. A proper choice of the degree of freedom is the roof displacement x_r . Assuming ϕ normalized with respect to x_r , the deflected shape \mathbf{x} of the MDOF system may be expressed as

$$\mathbf{x} = \phi x_r, \phi_r = 1 \quad (2)$$

Substituting Eq. (2) into Eq. (1) and pre-multiplying the resulting expression with ϕ^T gives the equation of motion of the ESDOF model in analogy to a real SDOF system,

$$L^* \ddot{D} + q^* = -L^* a_g \quad (3)$$

where D and q^* are the equivalent displacement and the force, respectively, of the ESDOF system,

$$D = \frac{m^*}{L^*} x_r, q^* = \phi^T \mathbf{q}, L^* = \phi^T \mathbf{M} \mathbf{r}, m^* = \phi^T \mathbf{M} \phi \quad (4), (5), (6), (7)$$

Structural (linear) damping is considered via a viscous damping ratio, which corresponds to the modal damping coefficient of the fundamental mode of the MDOF system.

The force-deformation relationship of the ESDOF system is determined from the base shear-roof displacement relationship of a nonlinear pushover analysis of the MDOF structure. Thereby, the nonlinear global pushover curves have to be idealized by a bilinear, trilinear, or multilinear diagram; see for example Fig. 1 for a bilinear idealization. Note that for the subsequent considerations the global pushover curves of the MDOF structure without gravity loads (i.e. no P-Delta) are utilized as the base case. The corresponding variables are indicated by a subscript "0", whereas parameters, which are effected by P-Delta are characterized by a subscript "p" (see also Fig. 1). The diagram needs to be translated into the force-deformation domain of the ESDOF model before it can be utilized for the ESDOF model analyses. The yield displacement D_y of the ESDOF system is obtained by multiplication of the roof displacement at yield x_{ry} with the ratio m^*/L^* (see Eq. (4)).

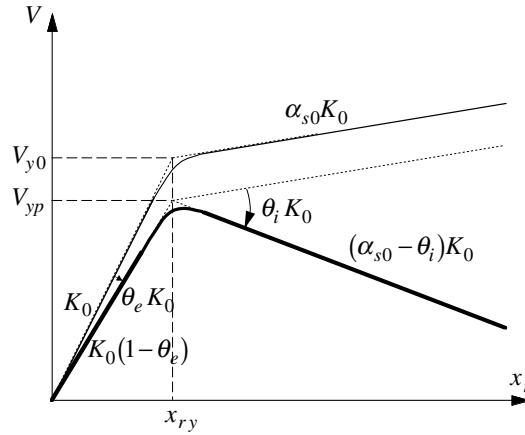


Figure 1: Global pushover curve of a MDOF structure with and without P-delta effects and its bilinear idealization.

The relation between the base shear V_0 and the equivalent force q^* is established following the procedure outlined subsequently. To satisfy static equilibrium the story force vector \mathbf{q}_0 and the vector of lateral loads applied to the MDOF structure in the pushover analysis must be equal:

$$\mathbf{q}_0 = \lambda \mathbf{R} \quad (8)$$

where \mathbf{R} is a vector (with arbitrary magnitude) proportional to the lateral loads, and the coefficient λ is a multiplier, which determines the magnitude of the lateral loads. Furthermore, the base shear V_0 is defined as the total sum of the story forces,

$$V_0 = \mathbf{1}^T \mathbf{q}_0 = \lambda \mathbf{1}^T \mathbf{R} \quad (9)$$

and thus, the relation between the equivalent force of the ESDOF system q_0^* and the base shear V_0 can be expressed by (compare also with Eq. (5)):

$$q_0^* = \beta V_0, \quad \beta = \frac{\boldsymbol{\phi}^T \mathbf{R}}{\mathbf{1}^T \mathbf{R}} \quad (10), (11)$$

The proposed procedure becomes identical with the approach of Fajfar [11], when the product of mass matrix and shape vector $\mathbf{M}\boldsymbol{\phi}$ and the distribution vector of the lateral load \mathbf{R} are proportional. The equivalent force q_{y0}^* at yield may be found by inserting the base shear at yield V_{y0} into Eq. (10). Utilizing the equivalent stiffness

$$k_0^* = \frac{q_{y0}^*}{D_y} \quad (12)$$

and “mass” L^* (compare with Eq. (6)), the initial (elastic) period of vibration of the ESDOF system can be computed from

$$T_0 = 2\pi \sqrt{\frac{L^* D_y}{q_{y0}^*}} \quad (13)$$

which may be different from the initial period of the actual MDOF system.

Representation of P-Delta in the ESDOF model

The impact of P-Delta on global pushover curves is illustrated in Fig. 1. It can be seen that the roof yield displacement x_{ry} is in general not substantially affected by P-Delta, however, elastic and post-yielding stiffness may decrease strongly (dependent on the magnitude of the gravity loads). Thus, P-Delta effects reduce the yield strength V_{yp} of the MDOF system and the yield strength q_{yp}^* of the ESDOF system, and the initial periods of vibration with and without P-Delta, T_p and T_0 , respectively, of the ESDOF model are related as:

$$T_p = T_0 \sqrt{\frac{1}{1 - \theta_e}} \quad (14)$$

because

$$q_{yp}^* = q_{y0}^* (1 - \theta_e) \quad (15)$$

In Eqs (14) and (15) θ_e represents the elastic stability coefficient.

P-Delta effects in SDOF systems should be represented by rotation of the hysteresis diagram. The question is what is the most appropriate stability coefficient (angle of rotation) to be employed. The P-Delta effect in MDOF systems depends on many aspects, including relative story strength and stiffness, distribution of gravity loads over the height, and the extent of inelastic behavior. It can be argued that in the elastic range of response the maximum story stability coefficient is most appropriate. However, in the inelastic range the P-Delta effect grows, and its importance strongly depends on the deflected shape of the structure, which varies with the extent of inelastic behavior. Thus, the maximum elastic story stability coefficient loses much of its meaning in the inelastic range and it may severely underestimate the importance of P-Delta effects.

The search for appropriate stability coefficients in ESDOF systems is a challenge partially addressed here. In this study, P-Delta effects are represented by the elastic and the inelastic stability coefficient, θ_e and θ_i , respectively, obtained from the global pushover curve, as shown in Fig. 1. The coefficients θ_e and θ_i are often different, but in an ESDOF system the rotation applies to both elastic and inelastic range. In general, θ_i is larger than θ_e . Therefore, the classical approach of rotating the entire hysteretic loop by means of θ_e may severely underestimate the effect of P-Delta on the structural response of the ESDOF model. Thus, the need exists to create an auxiliary backbone curve, whose rotation by an ‘‘auxiliary’’ stability coefficient θ_a results in the desired backbone curve including the P-Delta effect, but with the constraint that the auxiliary stability coefficient should be close to θ_i . The relations between the auxiliary backbone curve and the backbone curves of the equivalent ESDOF system with and without P-Delta are illustrated in Fig. 2. In the following a subscript ‘‘a’’ refers to properties of the auxiliary backbone curve. These properties are generated from the following conditions:

- The yield strength including P-Delta must be the same when determined from the actual (without P-Delta) and the auxiliary envelope:

$$q_{yp}^* = (1 - \theta_e) q_{y0}^* = (1 - \theta_a) q_{ya}^* \quad (16)$$

- The yield displacement is the same for all backbone curves, and may be expressed by the ratios of both auxiliary stiffness over auxiliary strength and actual stiffness over actual strength:

$$D_y = \frac{q_{y0}^*}{k_0^*} = \frac{q_{ya}^*}{k_a^*} \quad (17)$$

- The post-yielding stiffness including P-Delta effects is the same when calculated from the auxiliary envelope or the original backbone curve:

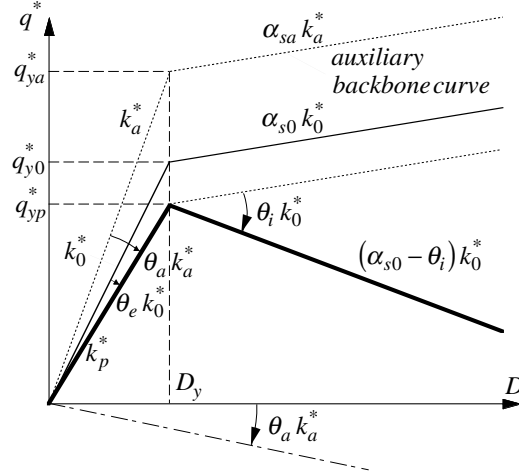


Figure 2: Global pushover curve in the ESDOF domain with and without P-delta effects and the corresponding auxiliary envelope.

$$(\alpha_{s0} - \theta_i)k_0^* = (\alpha_{sa} - \theta_a)k_a^* \quad (18)$$

- The strain hardening coefficient of the auxiliary backbone curve α_{sa} and of the original backbone curve (system without P-Delta) α_{s0} are identical:

$$\alpha_{s0} = \alpha_{sa} \quad (19)$$

The combination of Eqs (16) to (19) results in the following initial stiffness, yield strength, and stability coefficient of the auxiliary backbone curve:

$$k_a^* = \frac{1 - \theta_e + \theta_i - \alpha_{s0}}{1 - \alpha_{s0}} k_0^*, \quad q_{ya}^* = \frac{1 - \theta_e + \theta_i - \alpha_{s0}}{1 - \alpha_{s0}} q_{y0}^*, \quad \theta_a = \frac{\theta_i - \theta_e \alpha_{s0}}{1 - \theta_e + \theta_i - \alpha_{s0}} \quad (20)$$

Then, the period of vibration of the auxiliary ESDOF system is modified according to

$$T_a = T_0 \sqrt{\frac{1 - \alpha_{s0}}{1 - \theta_e + \theta_i - \alpha_{s0}}} \quad (21)$$

For backbone curves with small strain hardening coefficients ($\alpha_{s0} < 10\%$), the formulation can be condensed by assuming that the slope of the auxiliary backbone curve is equal to that of the original backbone curve (instead of using the same strain hardening coefficient of Eq. (19)):

$$k_0^* \alpha_{s0} = k_a^* \alpha_{sa} \quad (22)$$

This simplification does not lead to an appreciable loss of accuracy, and when Eqs (16) to (18) and (22) are combined, the following modified expressions are derived:

$$k_a^* = (1 - \theta_e + \theta_i) k_0^*, \quad q_{ya}^* = (1 - \theta_e + \theta_i) q_{y0}^*, \quad \alpha_{sa} = \frac{\alpha_{s0}}{1 - \theta_e + \theta_i}, \quad \theta_a = \frac{\theta_i}{1 - \theta_e + \theta_i}, \quad (23)$$

$$T_a = T_0 \sqrt{\frac{1}{1 - \theta_e + \theta_i}} \quad (24)$$

The yield reference displacement D_y and the parameters m^* and L^* remain unaltered in the auxiliary ESDOF system.

In earlier approaches dynamic P-Delta effects of SDOF systems may be considered only by rotating the hysteresis loop according to an elastic stability coefficient. The proposed use of an auxiliary backbone curve permits the direct use of the inelastic stability coefficient in the ESDOF analysis. Implementation requires that the SDOF analysis program either accommodates rotation of the hysteresis loop by an angle θ_a or permits incorporation of P-Delta effects corresponding to a gravity load that causes a stability coefficient θ_a .

Translation of results from the ESDOF domain into the MDOF domain

The results derived by means of an ESDOF model must be transformed back to the MDOF domain. For example, the equivalent displacement D is multiplied by the ratio L^*/m^* in order to describe an estimate of the roof displacement x_r of the actual MDOF structure, compare with Eq. (4). Results could be presented as normalized maximum peak roof displacement (Engineering Demand Parameter - EDP) versus an appropriate measure representing the intensity of the imposed ground motion (Intensity Measure - IM). For example, the parameter $[S_a(T_1)/g]/\gamma$ could be used as a relative intensity measure, where $S_a(T_1)$ is the spectral acceleration at the fundamental period of the MDOF structure (without P-Delta). The base shear strength coefficient γ , defined as $\gamma = V_{y0}/Mg$, is used to identify the strength of the structure [17]. The transfer of the relative intensity of the ground motion from the ESDOF into MDOF system domain is given by the relation:

$$\frac{S_a(T_1)/g}{\gamma} \equiv \frac{S_a(T_1)/g}{V_{y0}/Mg} = \frac{1}{\lambda_{IM}} \frac{S_a(T_1)/g}{q_{y0}^*/L^*g}, \quad \lambda_{IM} = \frac{L^*}{\beta M} \quad (25), (26)$$

If the maximum roof displacement x_r , normalized by the spectral displacement $S_d(T_1)$ is used as the EDP, the ESDOF to MDOF transformation is

$$\frac{x_r}{S_d} = \lambda_{EDP} \frac{D}{S_d}, \quad \lambda_{EDP} = \frac{L^*}{m^*} \quad (27), (28)$$

EVALUATION OF THE PROPOSED ESDOF SYSTEM

In this section the capability of the proposed ESDOF system to predict the collapse capacity of tall buildings is evaluated by numerical simulations. Assumptions and limitations are discussed.

Analyzed generic MDOF frame structures

For this study, two-dimensional regular generic multi-story single-bay frames of uniform story height are utilized. Medina [2] provides a detailed description of these structural models. They are composed of rigid beams, elastic flexible columns, and rotational springs at the beam ends. Nonlinear behavior at the component level is modeled by non-degrading elastic-plastic behavior of the rotational springs to represent the global cyclic response under seismic excitation. The bilinear hysteretic model is used throughout the study. The strength of the springs is tuned such that yielding is initiated simultaneously at all spring locations in a static pushover analysis under a parabolic (NEHRP, $k = 2$) design load pattern. To each joint of the frame an identical point mass is assigned. The bending stiffness of the columns and the stiffness of the springs are tuned to render a straight line fundamental mode shape. P-Delta effects are simulated by assigning identical gravity loads to each story. This implies that axial column forces due to gravity increase linearly from the top to the bottom of the frame. The considered structures have a fundamental period of vibration of $T_1 = 0.2N$ (N is number of stories), which makes them rather flexible and sensitive to P-Delta effects. The properties of the considered MDOF frame structures are as follows:

- Number of stories, $N = 12$ and 18
- Fundamental period, $T_1 = 2.4$ s for $N = 12$, and $T_1 = 3.6$ s for $N = 18$
- Base shear strength coefficient, $\gamma = 0.1$
- Strain hardening ratio of the springs, $\alpha = 0, 0.03$ and 0.06

- Percent of Rayleigh damping, $\zeta = 5\%$ of the first mode and the mode at which the cumulative mass participation exceeds 95%
- P/W ratio (ratio of dead load plus live load to dead load), $\vartheta = 1.4, 1.2$ and 1.0

Applied procedure

The following procedure is used to carry out a seismic evaluation of the collapse capacity of regular MDOF buildings utilizing ESDOF systems.

Ground motion records

A set of ordinary ground motion records (records without near-fault characteristics), denoted as LMSR-N, is utilized for time history analyses. The bin LMSR-N contains 40 ground motions recorded in Californian earthquakes of moment magnitude between 6.5 and 7 and closest distance to the fault rupture between 13 km and 40 km. These ground motions were recorded on NEHRP site class D (FEMA 368, 2000). Medina [2] selected the records of the bin LMSR-N from the PEER (Pacific Earthquake Engineering Research) Center Ground Motion Database. This set of ordinary records has strong motion duration characteristics that are not sensitive to magnitude and distance. Qualitatively, conclusions drawn from the seismic demand evaluation using this set of ground motions are expected to hold true also for stiffer soil and rock. A statistical evaluation of this bin of records and its detailed description are provided in [2].

Analysis and representation of the results

For a given structure with assigned geometric and structural properties, and a given ground motion record, a nonlinear time history analysis is performed. In the numerical simulations member P-delta effects and large displacement effects are not incorporated, because a pilot study revealed that both effects do not significantly affect the response even when dynamic instability is approached [18]. Utilizing ESDOF systems for collapse capacity prediction of tall buildings assumes implicitly that their seismic response is dominated by the first mode. Thus, the 5% damped spectral acceleration at the fundamental period $S_a(T_1)$ of the MDOF structure (without gravity loads) is selected as the IM. Results are presented as normalized maximum roof displacements versus the relative intensity $[S_a(T_1)/g]/\gamma$. The relative intensity $[S_a(T_1)/g]/\gamma$ is plotted on the vertical axis, and the maximum roof displacement x_r normalized by the spectral displacement $S_d(T_1)$ is plotted on the horizontal axis. In this representation a vertical line implies that x_r increases linearly with the ground motion intensity level $S_a(T_1)/g$. In the analysis process for a given structure and a given ground motion, the value of $[S_a(T_1)/g]/\gamma$ is increased in small increments of 0.25 until either a value of 15 is reached or dynamic instability is evident. The latter, which is synonymous to collapse, is assumed to occur when the relationship between the relative intensity $[S_a(T_1)/g]/\gamma$ and the normalized roof displacement approaches a zero slope. The normalized roof response to 40 ground motions provides a statistical representation of the response, which in subsequent graphs is represented by median values.

Evaluation and discussion of the results

Assessment of a 12 story MDOF structure

A 12 story frame with a fundamental period of vibration $T_1 = 2.4$ s is utilized to illustrate and evaluate the proposed procedure. The strain hardening ratio α at the element level (i.e. of the rotational springs) is 3%. A first story elastic stability coefficient of $\theta_{s1} = 0.084$ can be derived if the ratio ϑ of total dead + life load to total dead load (P/W ratio) acting on the first story level is 1.4. Specific data for the 12 story analysis cases are summarized in Tables 1 and 2.

Global pushover curves with and without P-Delta effects are obtained by application of a parabolic and an inverted triangular lateral load pattern, respectively. For this model the triangular load pattern is congruent to the shape of the first mode. In Fig. 3 global pushover curves for this structure are presented in non-dimensional form, using the base shear V_{y0} and the roof yield displacement x_{ry} of the system under parabolic load pattern without P-Delta effects for normalization. Heavy lines represent the nonlinear static response considering P-Delta, whereas thin lines refer to results without P-Delta effects. The global elastic

stiffness for the system under inverted triangular load is slightly larger than for the structure under parabolic load. This fact is also reflected in the period of vibration of the corresponding ESDOF systems; the period of the ESDOF model based on a parabolic load pattern is larger when identical shape vectors are applied (see Tables 1 and 2).

Table 1: Properties of ESDOF models based on global pushover under parabolic load pattern. 12 story generic frame: $T_1 = 2.4$ s, $\alpha = 3\%$, $\vartheta = 1.4$, $\theta_{s1} = 0.084$.

shape vector	α_{s0}	θ_e	θ_i	θ_a	α_{sa}	q_{ya}^* / q_{y0}^*	T_0	T_a	λ_{EDP}	λ_{IM}
linear	0.039	0.060	0.096	0.093	0.038	1.04	2.46	2.42	1.44	1.44
"1"							2.36	2.32	1.48	1.52
"2"							2.58	2.53	1.41	1.34
"3"							2.84	2.79	1.32	1.19

Table 2: Properties of ESDOF models based on global pushover under triangular load pattern. 12 story generic frame: $T_1 = 2.4$ s, $\alpha = 3\%$, $\vartheta = 1.4$, $\theta_{s1} = 0.084$.

shape vector	α_{s0}	θ_e	θ_i	θ_a	α_{sa}	q_{ya}^* / q_{y0}^*	T_0	T_a	λ_{EDP}	λ_{IM}
linear	0.045	0.062	0.094	0.091	0.044	1.03	2.40	2.36	1.44	1.28
"1"							2.32	2.28	1.43	1.38
"2"							2.50	2.46	1.38	1.24
"3"							2.74	2.70	1.29	1.10

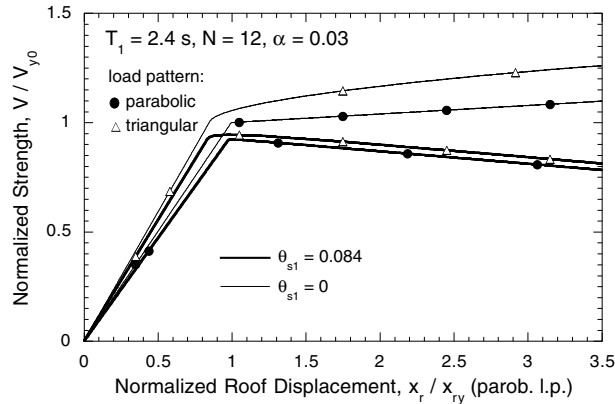


Figure 3: Global pushover curves based on parabolic and triangular load pattern, 12-story frame with and without P-delta effects.

For a parabolic load pattern the post-yielding slope is linear, which is a result of tuning the yield strength to this load pattern. A strain hardening ratio α of 3% for the rotational springs render global strain hardening ratios α_{s0} of 3.9% (parabolic load) and 4.5% (in average for inverted triangular load), respectively. P-Delta effects cause the nonlinear static response to have a negative post-yield slope. For the considered building the global stability coefficient in the inelastic branch of deformation θ_i ($\approx 9-10\%$) is approximately 50% larger than the global elastic stability coefficient θ_e ($\approx 6\%$). The inelastic slopes (including the effect of P-Delta) are parallel for both load patterns. In Tables 1 and 2 the stability coefficient θ_a and the slope α_{sa} of the auxiliary backbone curve derived from Eq. (23) are given. Note that for this structure with a moderate negative post-yielding roof displacement slope the stability coefficient of the auxiliary backbone curve is slightly smaller than the inelastic stability coefficient.

In Figs 4 and 5 the normalized displacement profiles at discrete roof displacements are shown. The profiles of Fig. 4 belong to the 12 story building under a parabolic load pattern. The normalized elastic deflected shapes of a static analysis with and without considering P-Delta effects (denoted by "1") are almost identical and close to a straight line. Driving the building in its inelastic range of deformation does not change the shape of the profile significantly when P-Delta effects are neglected (see the profiles denoted by "2" and "3" - light lines). However, the consideration of P-Delta leads to a "belly" in the inelastic profiles "2" and "3", indicating that there is a concentration of the story drifts in the lower stories. In Fig. 5 profiles of the same building exposed to a triangular load are presented. Here, the difference in the inelastic profiles "2" and "3" of a static analysis with and without P-Delta is less pronounced.

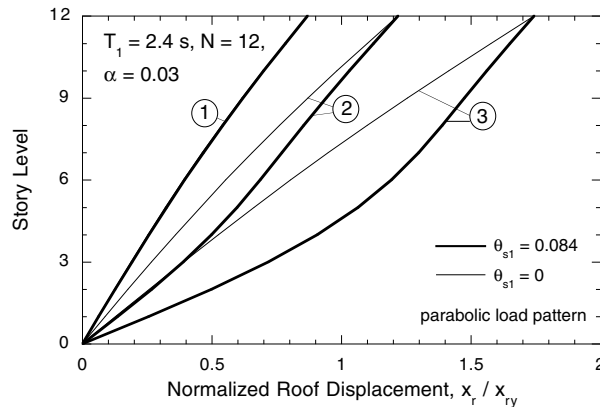


Figure 4: Deflected shapes from pushover analysis based on parabolic load pattern, 12-story frame with and without P-delta effects.

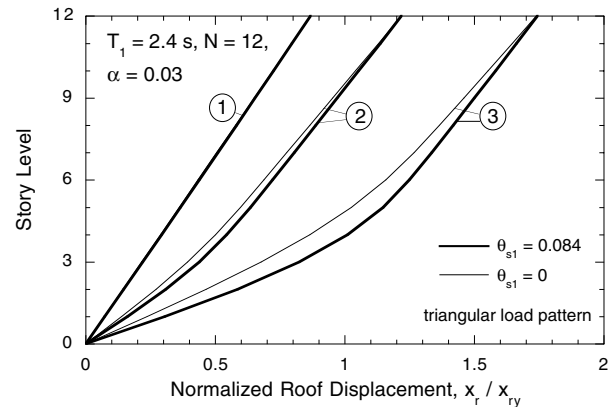


Figure 5: Deflected shapes from pushover analysis based on triangular load pattern, 12-story frame with and without P-delta effects.

Displacement profiles "1", "2" and "3" with P-Delta are subsequently utilized as shape vectors ϕ , which enter the properties of the ESDOF systems for deriving the nonlinear dynamic response of these structures subjected to ordinary ground motions. Additionally, a linear shape vector, which coincides with the first mode of the considered MDOF structures, is selected to model the ESDOF system.

In Tables 1 and 2 the properties of all ESDOF models are summarized, based on parabolic and triangular load patterns and on different shape vectors. It can be seen that the period T_0 of the ESDOF system is close to the fundamental period T_1 of the corresponding MDOF structure when a linear or "elastic" shape vector is utilized. Inelastic profiles "2" and "3" lead to a softening of the ESDOF system. The scaling coefficients λ_{EDP} and λ_{IM} according to Eqs (26) and (28), respectively, are also given in these Tables.

Fig. 6 shows the results of sets of IDA analyses applied to these ESDOF models based on the pushover with parabolic load pattern. The median response of the ESDOF models is presented in the MDOF domain. Heavy lines represent ESDOF results considering P-Delta effects, and light lines refer to outcomes disregarding P-Delta. When a curve becomes horizontal the collapse capacity of the corresponding ESDOF model is attained. Depending on the choice of the shape vector, ESDOF systems predict dynamic instability due to P-Delta between relative intensities $[S_a(T_1)/g]/\gamma$ of 8.5 and 10.3. Comparison with the "exact" median of the relative collapse intensity ($[S_a(T_1)/g]/\gamma = 9.7$) from IDAs of the actual MDOF structure (shown by a dashed line) reveals that all ESDOF systems, even though they are based on different shape vectors, provide a reasonable estimate of the collapse capacity. The ESDOF system derived from shape vector "3" overestimates slightly the collapse capacity, whereas the equivalent system based on the elastic displacement profile underestimate its actual value. The dispersion of the ESDOF median response predictions utilizing various shape vectors is narrow banded for analyses without P-Delta, and also for moderate inelastic systems considering P-Delta when the relative intensity

$[S_a(T_1)/g]/\gamma$ is smaller than about 5. For this model, P-Delta effects do not have a pronounced influence on the system behavior at relative intensities ($[S_a(T_1)/g]/\gamma$ lower than about 3.5).

In Fig. 7 medians of peak roof displacements are presented when the properties of the ESDOF systems are based on a pushover analysis with triangular load distribution. The maximum roof drift demands are very similar to the predictions shown in Fig. 6 (parabolic load pattern): dynamic instabilities occur between relative intensities of 9.3 and 10.3. This confirms findings of earlier investigations (see e.g. [12]) that the results derived from ESDOF systems are insensitive to the choice of the load pattern in the underlying pushover analyses.

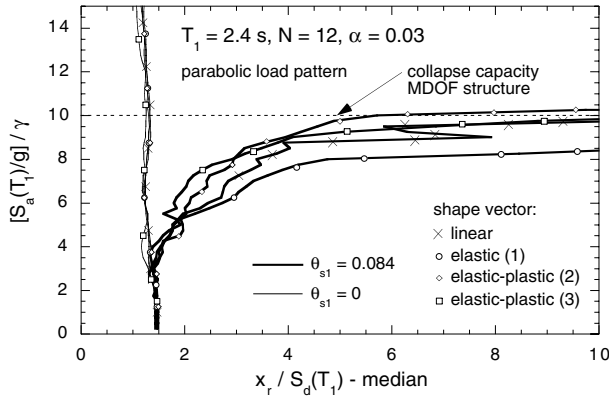


Figure 6: Effect of different shape vectors on the median normalized max. roof drift prediction with ESDOF model, 12 story frame with and without P-delta effects, underlying pushover with parabolic load pattern.

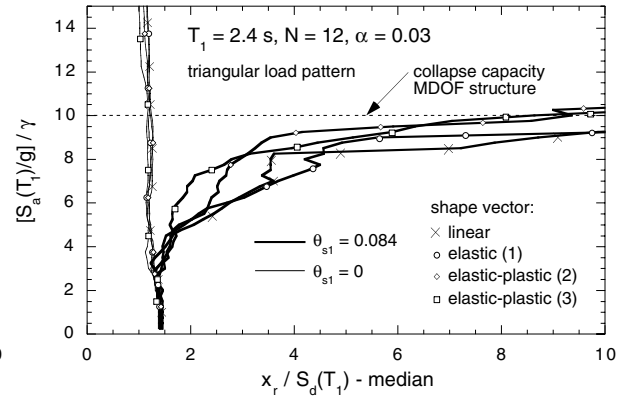


Figure 7: Effect of different shape vectors on the median normalized max. roof drift prediction with ESDOF model, 12 story frame with and without P-delta effects, underlying pushover with triangular load pattern.

Assessment of a 18 story MDOF structure

The proposed procedure is tested also for a 18 story 3.6 s single-bay frame structure, which is more sensitive to P-Delta effects. The strain hardening coefficient α of the bilinear springs is 3%, and the P/W ratio ϑ is selected to be 1.4. P-Delta has a severe impact on this building, which is reflected by a first story elastic stability coefficient of $\theta_{s1} = 0.130$. Specific data for the 18 story analysis cases are summarized in Tables 3 and 4.

Table 3: Properties of ESDOF models based on global pushover under parabolic load pattern. 18 story generic frame: $T_1 = 3.6$ s, $\alpha = 3\%$, $\vartheta = 1.4$, $\theta_{s1} = 0.130$.

shape vector	α_{s0}	θ_e	θ_i	θ_a	α_{sa}	q_{ya}^* / q_{y0}^*	T_0	T_a	λ_{EDP}	λ_{IM}
linear	0.040	0.092	0.370	0.290	0.031	1.28	3.69	3.26	1.46	1.46
"1"							3.46	3.06	1.50	1.62
"2"							4.01	3.55	1.39	1.30
"3"							4.69	4.14	1.23	1.08

Table 4: Properties of ESDOF models based on global pushover under triangular load pattern. 18 story generic frame: $T_1 = 3.6$ s, $\alpha = 3\%$, $\vartheta = 1.4$, $\theta_{s1} = 0.130$.

shape vector	α_{s0}	θ_e	θ_i	θ_a	α_{sa}	q_{ya}^* / q_{y0}^*	T_0	T_a	λ_{EDP}	λ_{IM}
linear	0.083	0.091	0.354	0.280	0.065	1.26	3.60	3.20	1.46	1.30
"1"							3.54	3.15	1.45	1.36
"2"							3.84	3.42	1.42	1.18
"3"							4.16	3.70	1.34	1.07

In Fig. 8 global pushover curves for parabolic and inverted triangular load patterns are presented. The shapes of the curves resemble those of the 12 story building, however P-Delta effects are much more pronounced. The inelastic stability coefficient ($\theta_i \approx 35\text{-}37\%$) is about four times larger than the elastic one ($\theta_e \approx 9\%$). The static roof displacement at collapse is only 3.6 times the roof yield displacement (parabolic load pattern). A 3% strain hardening ratio at the spring level results in 4.0% global strain hardening for the parabolic load pattern and in about 8% for an inverted triangular load pattern. Selected displacement profiles for a parabolic load pattern are shown in Fig. 9. In addition to a linear function these profiles (with P-Delta) are utilized as shape vectors for modeling the ESDOF systems. In Tables 3 and 4 the properties of the ESDOF models and the auxiliary parameters according to Eqs (23) and (24) based on parabolic and triangular loading, respectively, are recorded.

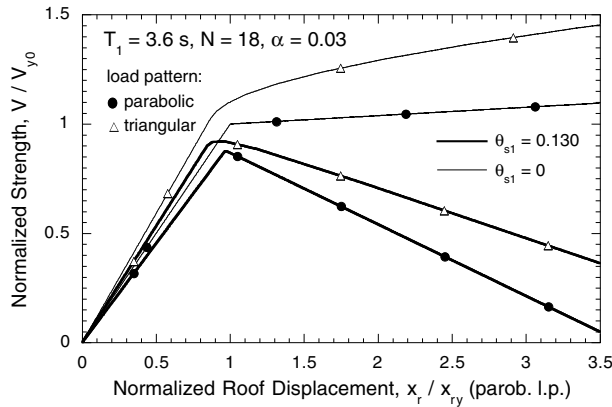


Figure 8: Global pushover curves based on parabolic and triangular load pattern, 18-story frame with and without P-delta effects.

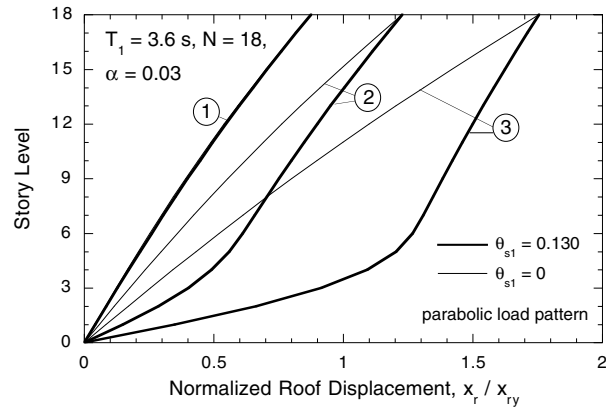


Figure 9: Deflected shapes from pushover analysis based on parabolic load pattern, 18-story frame with and without P-delta effects.

Fig. 10 represents medians of the peak roof displacements derived from 40 IDA analyses for ESDOF systems with different shape vectors. According to a study on the MDOF structure, dynamic instability occurs at a relative intensity $[S_a(T_1) / g] / \gamma$ of 3.4. Time history analyses using ESDOF systems predict this phenomenon at median intensities between 2.8 and 3.4. As for the 12 story structure, an ESDOF system based on the elastic-plastic deformation profile "3" leads to a higher estimate of the collapse intensity compared the outcomes utilizing shape vector based on a linear or elastic deflected profile. However, all ESDOF models based on different shape vectors result in a reasonable approximation of the collapse capacity. As shown in Fig. 11, ESDOF systems based on pushover outcomes with underlying inverted triangular load pattern also render estimates of about the collapse capacity of the same magnitude.

A similar example is developed by varying the strain hardening ratio at the spring level: α is stepwise increased from 0% to 3% to 6%. The ESDOF model used in the analyses is based on a parabolic pushover load and the inelastic shape vector "3". From Fig. 12 it can be observed that deviations between maximum

roof drift predictions with and without P-Delta effects are initiated at the same relative ground motion intensity $[S_a(T_1)/g]/\gamma$ of approximately 2 for all structures with different α , however the gradient and the rate of dynamic collapse depends strongly on the spring strain hardening ratio. Naturally the collapse capacity is largest for $\alpha = 6\%$ and smallest for $\alpha = 0$. The results of Fig. 12 indicate also that predictions of the collapse capacity with ESDOF systems are mostly on the conservative side.

In another study the influence of the P/W ratio ϑ on the quality of the collapse capacity predictions by means of ESDOF models is evaluated. Figure 13 shows stability coefficients as well as MDOF and ESDOF collapse capacities for P/W ratios of 1.4, 1.2 and 1.0 ($\theta_{s1} = 0.13, 0.111, \text{ and } 0.093$, respectively). Observe the large effect of the P/W ratio on the collapse capacity of the MDOF structure, which may lead to differences of almost 60% depending on the additional live load included in the gravity load acting on the structure.

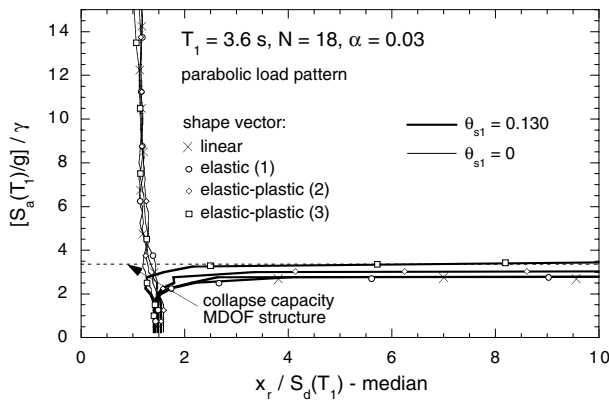


Figure 10: Effect of different shape vectors on the median normalized max. roof drift prediction with ESDOF model, 18-story frame with and without P-delta effects, underlying pushover with parabolic load pattern.

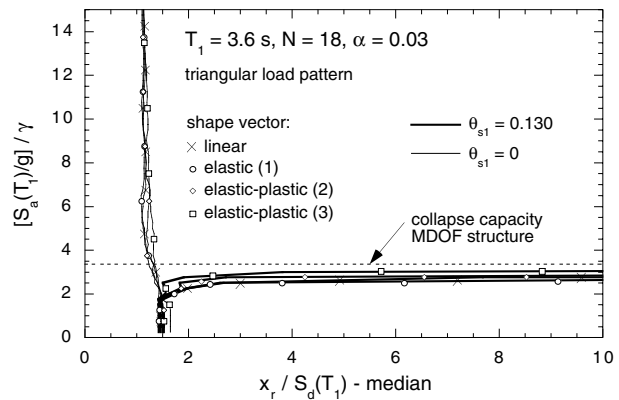


Figure 11: Effect of different shape vectors on the median normalized max. roof drift prediction with ESDOF model, 18-story frame with and without P-delta effects, underlying pushover with triangular load pattern.

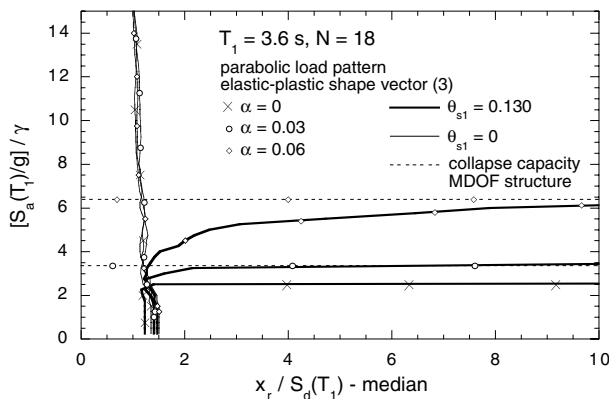


Figure 12: Effect of different strain hardening ratios on the median normalized max. roof drift prediction with ESDOF model, 18 story frame with and without P-delta effects, underlying pushover with parabolic load pattern.

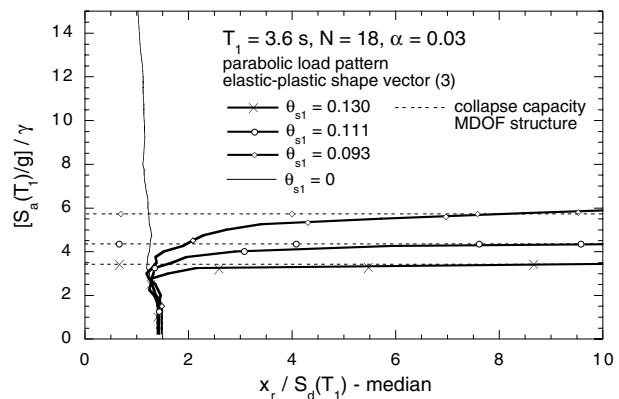


Figure 13: Effect of different gravity loads on the median normalized max. roof drift prediction with ESDOF model, 18 story frame with and without P-delta effects, underlying pushover with parabolic load pattern.

SUMMARY OF PROCEDURE TO ESTIMATE THE COLLAPSE CAPACITY OF MDOF STRUCTURES UTILIZING ESDOF SYSTEMS

The results presented here demonstrate that global P-Delta effects for non-deteriorating MDOF frame structures can be predicted with good accuracy from ESDOF systems using the following procedure:

- Perform global pushover analyses of the MDOF structure, with and without considering P-Delta effects, to obtain global pushover properties and elastic and inelastic stability coefficients. It is recommended to select an inverted triangular or parabolic load pattern.
- From the properties of the MDOF structure derive the auxiliary backbone curve and the auxiliary stability coefficient for the ESDOF system.
- Select a shape vector according to the first mode or according to the elastic static deflection of the MDOF structure obtained from the pushover analysis. Determine the parameters of the ESDOF system, such as mass, stiffness, period etc.
- Assign a constitutive law (hysteretic loop) to the ESDOF system, which represents, in the average, the nonlinear response characteristics of the MDOF structure.
- Predict the time history response in the ESDOF domain, using the auxiliary backbone curve and stability coefficient, and transform the response back to the MDOF domain.
- The collapse capacity can be obtained from a statistical evaluation of ESDOF data, with the results to be scaled up to the MDOF domain. Advantage can be taken of statistical data available on this parameter for ESDOF systems of appropriate properties, such as those presented in Ref. [6].

CONCLUSIONS

The results presented in this study suggest that the application of the proposed ESDOF systems is appropriate to estimate P-Delta effects in non-deteriorating regular MDOF structures. In most cases the results derived from ESDOF systems for P-Delta collapse capacities are conservative; in particular if elastic deformation profiles are used as shape vectors. The initial period of the ESDOF depends on the load pattern and deformation profile of the underlying pushover. An overview of the dispersion of the results can be found by application of various proposed load patterns and shape vectors. Reviewing the results obtained in this study reveals that this dispersion decreases as the effect of P-Delta on the nonlinear response increases.

ACKNOWLEDGEMENTS

This research was carried out as part of a comprehensive effort at Stanford's John A. Blume Earthquake Engineering Center to assess seismic demands for frame structures. This effort is supported by the Pacific Earthquake Engineering Research (PEER) Center. C. Adam received for his research at Stanford University a fellowship from the *Max Kade Foundation, Inc.* The studies of L.F. Ibarra were mainly supported by the Consejo Nacional de Ciencia y Tecnologia (CONACYT) and complemented by funds from PEER. All this support is gratefully acknowledged.

REFERENCES

1. Gupta, A., Krawinkler, H. "Seismic demands for performance evaluation of steel moment resisting frame structures." Report No. 132. Stanford: John A. Blume Earthquake Engineering Center, Stanford University, 1999.
2. Medina R. "Seismic demands for nondeteriorating frame structures and their dependence on ground motions." Ph.D. Dissertation submitted to the Department of Civil and Environmental Engineering. Stanford: Stanford University, 2002.

3. Vian, D., Bruneau, M. "Experimental investigation of P-delta effects to collapse during earthquakes." Technical Report MCEER-01-0001. Buffalo: MCEER, University of Buffalo, 2002.
4. Williamson, E.B. "Evaluation of damage and P-delta effects for systems under earthquake excitation." *Journal of Structural Engineering* 2003; 129: 1036-1046.
5. Aschheim, M, Montes, E.H. "The representation of P-delta effects using yield point spectra." *Engineering Structures* 2003; 25: 1387-1396.
6. Ibarra, L.F. "Global collapse of frame structures under seismic excitations." Ph.D. Dissertation submitted to the Department of Civil and Environmental Engineering. Stanford: Stanford University, 2003.
7. Fajfar, P., Fischinger, M. "N2 - a method for non-linear seismic analysis of regular buildings." Proc. 9th World Conference on Earthquake Engineering, August 2-9, 1988, Tokyo-Kyoto, Japan, pp. V-111 - V-116, 1988.
8. Qi, X., Moehle J.P. "Displacement design approach for reinforced concrete structures subjected to earthquakes" Report No. UCB/EERC-91/02. Berkeley: Earthquake Engineering Research Center, University of California, 1991.
9. Kuramoto, H., Teshigawara, M. "Prediction of earthquake response of buildings using equivalent single-degree-of-freedom system." Proc. US-Japan Workshop on Performance-Based Earthquake Engineering Methodology for Reinforced Concrete Building Structures, PEER Report, 1999/10, pp. 53-67, 1999.
10. Chou Chung-Che "An energy-based seismic evaluation procedure for moment resisting frames." Ph.D. Dissertation. San Diego: University of California, 2001.
11. Fajfar, P. "Structural analysis in earthquake engineering - a breakthrough of simplified non-linear methods." Proc. 12th European Conference on Earthquake Engineering September 9-13, 2002, London, UK, CD-ROM paper, Paper Ref. 843, 20 pp. Elsevier, 2002.
12. Bernal, D. "Instability of buildings subjected to earthquakes." *Journal of Structural Engineering* 1992; 118: 2239-2260.
13. Aydinoglu, M. N. "Inelastic seismic response analysis based on story pushover curves including P-delta effects." Report No. 2001/1, KOERI. Istanbul: Department of Earthquake Engineering, Bogazici University, 2001.
14. ATC-40, Applied Technology Council, "Seismic evaluation and retrofit of concrete buildings." Report No. SSC 96-01. Redwood City: Seismic Safety Commission, 1996.
15. FEMA-356, "Prestandard and commentary for the seismic rehabilitation of buildings." Washington D.C.: Federal Emergency Management Agency, 2000.
16. Bernal, D. "Instability of buildings during seismic response." *Engineering Structures* 1998; 20: 496-502.
17. Alavi, B., Krawinkler, H. "Effects of near-fault ground motions on frame structures." Report No. 138. Stanford: The John A. Blume Earthquake Engineering Center, Stanford University, 2001.
18. Adam, C., Krawinkler, H. "Large displacements of elastic-plastic frame structures exposed to pulse-type ground motion." Proc. Response of Structures to Extreme Loading 2003 (XL2003), August 3 - 6, 2003, Toronto, Canada, CD-ROM paper, 8 pp. Elsevier, 2003.